



Focused exhumation along megathrust splay faults in Prince William Sound, Alaska



Peter J. Haeussler ^{a,*}, Phillip A. Armstrong ^b, Lee M. Liberty ^c, Kelly M. Ferguson ^b,
Shaun P. Finn ^c, Jeanette C. Arkle ^b, Thomas L. Pratt ^d

^a United States Geological Survey, 4210 University Dr., Anchorage, AK 99508, United States

^b Geological Sciences, California State University—Fullerton, 800 N. State College Boulevard, Fullerton CA 92834, United States

^c Department of Geosciences, Boise State University, 1910 University Dr., Boise, ID 83725, United States

^d United States Geological Survey, 12201 Sunrise Valley Drive, M.S. 905, Reston, VA 20192, United States

ARTICLE INFO

Article history:

Received 10 June 2014

Received in revised form

7 October 2014

Accepted 13 October 2014

Available online 7 November 2014

Keywords:

Megathrust splay faults

Rapid exhumation

Alaska

Underplating

Thermochronology

1964 Great Alaska earthquake

Accretionary prisms

ABSTRACT

Megathrust splay faults are a common feature of accretionary prisms and can be important for generating tsunamis during some subduction zone earthquakes. Here we provide new evidence from Alaska that megathrust splay faults have been conduits for focused exhumation in the last 5 Ma. In most of central Prince William Sound, published and new low-temperature thermochronology data indicate little to no permanent rock uplift over tens of thousands of earthquake cycles. However, in southern Prince William Sound on Montague Island, apatite (U-Th)/He ages are as young as 1.1 Ma indicating focused and rapid rock uplift. Montague Island lies in the hanging wall of the Patton Bay megathrust splay fault system, which ruptured during the 1964 M9.2 earthquake and produced ~9 m of vertical uplift. Recent geochronology and thermochronology studies show rapid exhumation within the last 5 Ma in a pattern similar to the coseismic uplift in the 1964 earthquake, demonstrating that splay fault slip is a long term (3–5 my) phenomena. The region of slower exhumation correlates with rocks that are older and metamorphosed and constitute a mechanically strong backstop. The region of rapid exhumation consists of much younger and weakly metamorphosed rocks, which we infer are mechanically weak. The region of rapid exhumation is separated from the region of slow exhumation by the newly identified Montague Strait Fault. New sparker high-resolution bathymetry, seismic reflection profiles, and a 2012 M_w4.8 earthquake show this feature as a 75-km-long high-angle active normal fault. There are numerous smaller active normal(?) faults in the region between the Montague Strait Fault and the splay faults. We interpret this hanging wall extension as developing between the rapidly uplifting sliver of younger and weaker rocks on Montague Island from the essentially fixed region to the north. Deep seismic reflection profiles show the splay faults root into the subduction megathrust where there is probable underplating. Thus the exhumation and extension in the hanging wall are likely driven by underplating along the megathrust décollement, thickening in the overriding plate and a change in rheology at the Montague Strait Fault to form a structural backstop. A comparison with other megathrust splay faults around the world shows they have significant variability in their characteristics, and the conditions for their formation are not particularly unique.

Published by Elsevier Ltd. This is an open access article under the CC BY license (<http://creativecommons.org/licenses/by/3.0/>).

1. Introduction

Thrust faults that splay upward off of the seismogenic part of the subduction zone décollement, herein referred to as megathrust splay faults, have received considerable attention in recent years for their role in tsunami generation. These splay faults have been implicated in generating deadly tsunamis during earthquakes, for

example, the 1932 Mexico ([Okal and Borrero, 2011](#)), 1944 Tonankai ([Park et al., 2000, 2002; Baba et al., 2006; Moore et al., 2007a,b](#)), 1945 Makran ([Heidarzadeh et al., 2008](#)), 1964 Alaska ([Plafker, 1969](#)), and 2010 Ecuador ([Collot et al., 2008](#)). Moreover, theoretical studies identify splay faults as particularly effective in generating local tsunamis (e.g., [Wendt et al., 2009](#)).

The 1964 M9.2 earthquake in Alaska was the birthplace of the concept of a subduction megathrust as well as megathrust splay faults ([Plafker, 1969](#)). [Plafker \(1967, 1969\)](#) identified the Patton Bay megathrust splay fault as the source of the local tsunami that inundated the town of Seward about 30 min after the earthquake ([Figs. 1 and 2](#)).

* Corresponding author. Tel.: +1 907 786 7447.

E-mail address: pheuslr@usgs.gov (P.J. Haeussler).

Although megathrust splay faults, or more commonly, out-of-sequence active thrust faults within accretionary prisms, have been found throughout the world, their characteristics (e.g. geometry, location, slip history, role in wedge development) are not generally known. In this paper we present evidence for rapid rock uplift along the Patton Bay megathrust splay fault system in Alaska, describe the structure of the fault system, and briefly compare this system to other megathrust splay fault systems.

2. The 1964 Alaska earthquake and the Patton Bay Fault system

The M9.2 1964 Great Alaska earthquake remains the second-largest instrumentally recorded earthquake (e.g. Johnson et al., 1996; Ichinose et al., 2007). There is an exceptionally good record of coseismic uplift and subsidence during this earthquake because of the large number of islands and the vast length of coastline in the rupture area (Plafker, 1969; Figs. 1 and 2). The earthquake ruptured an area roughly 800 km long and up to 250 km wide, with two areas of concentrated moment release beneath Prince William Sound and near Kodiak Island (Johnson et al., 1996; Ichinose et al., 2007; Suito and Freymueller, 2009). Early Tertiary Pacific plate oceanic crust is being subducted beneath Kodiak Island, but it is thick oceanic-plateau like crust of the Yakutat terrane that is being subducted beneath Prince William Sound (Eberhart-Phillips et al., 2006; Christeson et al., 2010; Fig. 1). Horizontal displacements in Prince William Sound reached 20 m at the surface, and slip along the megathrust fault plane has been modeled as up to 40 m (Christenson and Beck, 1994; Holdahl and Sauber, 1994; Johnson et al., 1996; Ichinose et al., 2007). Plafker (1967, 1969) mapped surface rupture on two megathrust splay faults on Montague Island in southern Prince William Sound (Figs. 2 and 3). The principal fault is the Patton Bay Fault, which he inferred to extend most of the length of Montague Island and farther southwest to offshore of the town of Seward. The shoreline of Montague Island was raised up to 9 m by motion on the Patton Bay Fault, and the maximum fault slip was measured as 8 m. The smaller Hanning Bay thrust fault lies 10 km northwest of, and in the hanging wall of, the Patton Bay Fault. It also

ruptured in the 1964 earthquake and had up to 7 m of slip. Lastly, the footwall of the Patton Bay thrust was also uplifted 5 m on Montague Island, which indicates another thrust fault lies beneath the Patton Bay thrust. A 70-km-long scarp associated with this lower fault, which we refer to as the Cape Cleare Fault, is clearly imaged offshore southwest of Montague Island on a compilation of bathymetric surveys (Fig. 2) and in our new high-resolution seismic reflection data (Liberty et al., 2013). This fault may constitute a left step-over in the fault system. Collectively, we refer to these thrusts as the Patton Bay megathrust splay fault system. Lastly, Plafker (1969) inferred a separate megathrust splay fault lies beneath Middleton Island, which is located about ~80 km southeast of Montague Island, because it was uplifted 3.4 m in the 1964 earthquake.

Plafker (1969) inferred that a southwestern extension of the Patton Bay megathrust splay fault system caused the tsunami that hit the town of Seward about 30 min after the 1964 earthquake (Fig. 2; Wilson and Tørum, 1972). Plafker (1969) noted that tsunami arrival times were consistent with a source that is located along strike from the mapped Patton Bay thrust (which we now understand to be the Cape Cleare Fault), and were too early to be from a source located farther toward the trench (see also Suleimani et al., 2010). Therefore, in a historical context, the Patton Bay thrust was the first identified megathrust splay fault, and it was interpreted as tsunamigenic (Plafker, 1969).

Megathrust splay faults that sole into the subduction zone décollement were imaged on USGS Trans Alaska Crustal Transect (TACT) deep seismic reflection data collected in 1988. Refraction profiles and interpretations were previously published (Brocher et al., 1994; Fuis et al., 2008), and aspects of the reflection profiles are shown in Liberty et al. (2013). TACT profile B generally trends northwesterly across the strike of structures and shows the décollement and two megathrust splay fault systems (Figs. 2, 3A and 3B). One splay fault was imaged beneath Middleton Island, another beneath Wessels Reef. The principal conclusion from the imaging is that the faults clearly branch from the subduction décollement at a low angle. Also, the splay faults steepen upward within 2–6 km above the décollement. Although the TACT B profile¹ does not extend to the north across the Patton Bay Fault, it is reasonable to infer that it has similar structural characteristics.

The TACT Prince William Sound (PWS) profile reveals underplating, shortening, and splay fault geometry beneath Montague Straight (Figs. 2, 3C, 3D, 3E). This NE–SW trending profile extends along Montague Strait, and is oriented at a low angle to the strike of the splay faults, which makes the line geometry less than ideal for simple visualization. Nonetheless, there are prominent fault-plane reflections from the Hanning Bay, Patton Bay, and Cape Clear Faults that parallel each other and extend to near the décollement (Liberty et al., 2013). Although these reflections are almost certainly out-of-plane, they still demonstrate that all three faults extend close to the décollement. Moreover, the profile shows a band of strong reflections along the décollement in the region below Montague Strait. Just above the décollement are sub-horizontal reflectors that we interpret as fault-bounded duplexes (Fig. 3E). Although the survey does not have the resolution to image the interior structure of these features, this geometry is similar to deep underplating as interpreted elsewhere along the Alaskan continental margin (Moore et al., 1991; Gutscher et al., 1998) where laterally continuous strong reflectors 5+ km long are observed at or above the subduction décollement. Moreover, velocity models from the refraction data (Brocher et al., 1994) along this line show a distinct 2 km step up in higher velocity material at the

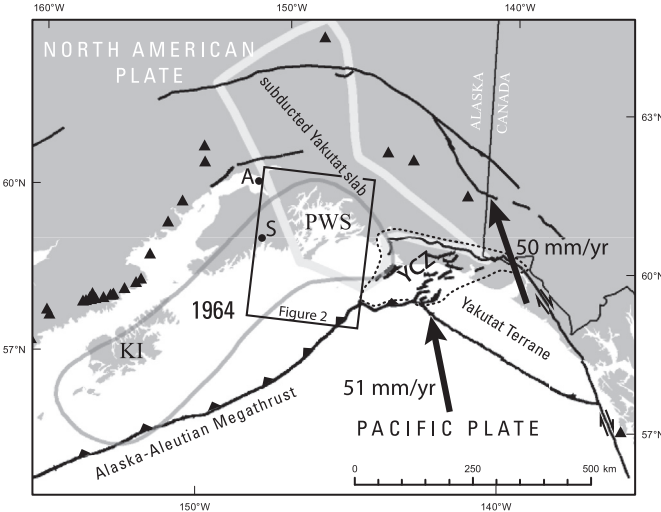


Fig. 1. Map of tectonic setting of south-central Alaska. The rupture area of the 1964 earthquake is shown with the thin gray line and 1964 label. Triangles show locations of volcanoes. The extent of the subducted Yakutat slab is from Eberhart-Phillips et al. (2006). Major active faults from the compilation of Plafker et al. (1994). Yakutat–North America plate velocity from Elliott et al. (2010). Pacific–North America plate velocity from Plattner et al. (2007). Labels: Prince William Sound, PWS; Kodiak Island, KI; Seward, S; Anchorage, A. Dotted line surrounds the leading edge of the Yakutat collision zone (or Saint Elias orogen), labeled YCZ.

¹ TACT profiles C and D are located further north in Prince William Sound, but they only weakly image the décollement and do not reveal the deep structure of any additional faults.

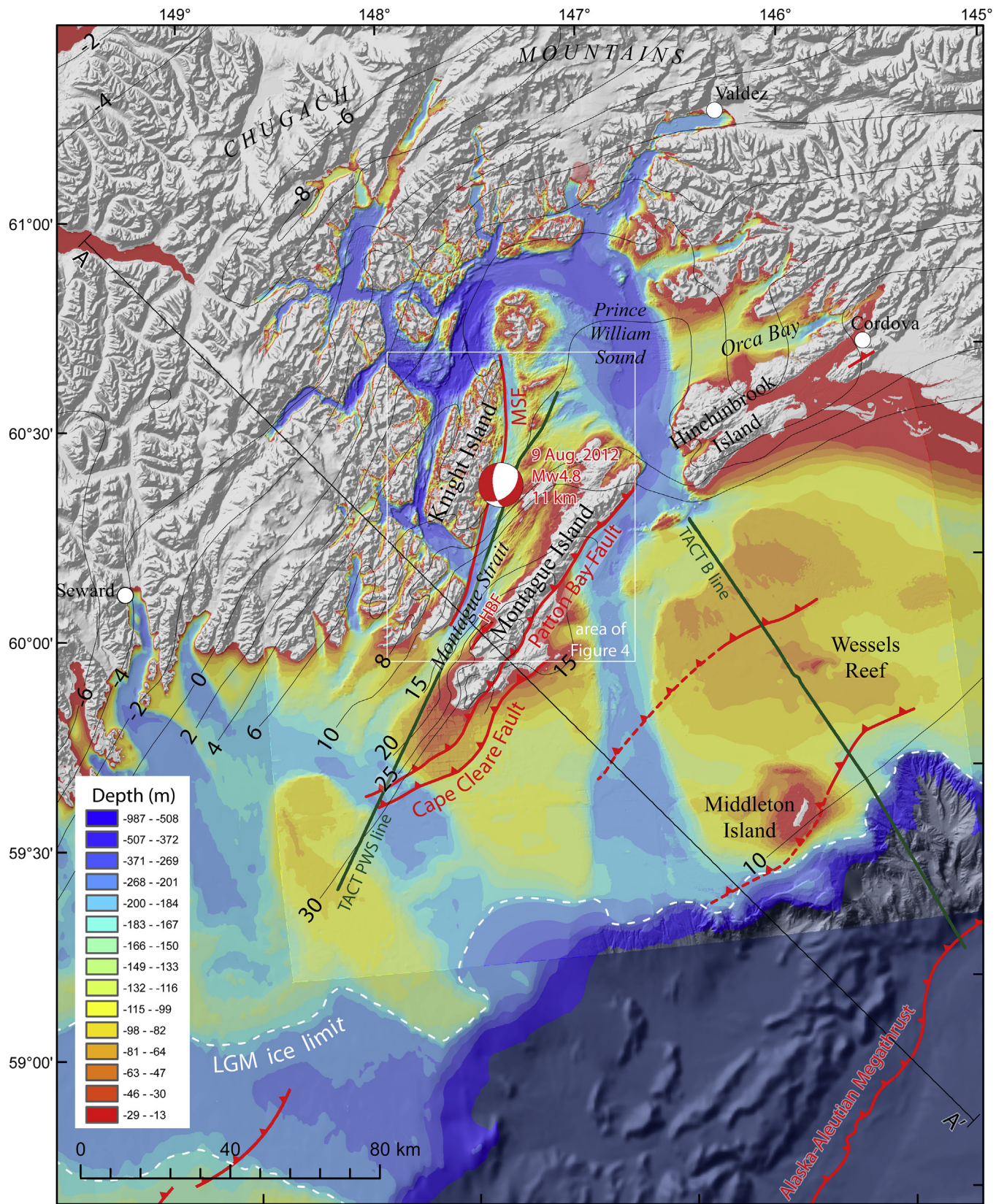


Fig. 2. Map focused on Prince William Sound showing active faults and crustal deformation during the 1964 earthquake. Topography is a greyscale hillshade. Bathymetry data from NOAA compilation, illumination is from the northwest. Active faults, in red, are from compilation of Plafker et al. (1994) and from our work. HBF, Hanning Bay fault; MSF, Montague Strait fault. Uplift and subsidence contours, in black, are in units of feet as originally mapped by Plafker (1969). Dashed white line is our inferred Last Glacial Maximum (LGM) ice limit. Green lines show the location of the TACT deep seismic profiles discussed in the text. Cross section along line A–A' is shown in Fig. 7. (For interpretation of the references to color in this figure legend, the reader is referred to the web version of this article.)

same location (Fig. 3D). The combination of the duplexing along the décollement along with the shortening across the Patton Bay Fault system would inevitably lead to surface uplift.

To better characterize the near-surface expression of the splay fault systems, we collected 1200 km of high-resolution seismic reflection data (see also Liberty et al., 2013; Fig. 4). We used 300–500 J sparker sources and single and multichannel recording streamers. Methods and details of data processing are shown in Liberty et al. (2013), but that paper does not present the images from the region of Montague Strait, shown here (Figs. 4 and 5). The data show a Holocene and Quaternary section of unconsolidated strata up to 500-m thick above the Tertiary Orca Group basement rocks, as well as numerous fault traces that displace shallow strata and the Holocene sediments and sea floor (Fig. 5).

One of the principal targets for imaging was a fault scarp along the northwest side of Montague Strait. This scarp, which we refer to as the Montague Strait Fault,² is clearly imaged as a sea-bottom scarp on NOAA (National Oceanographic and Atmospheric Administration) multibeam surveys (Fig. 4). This fault scarp is the longest and largest sea-bottom scarp in all of Prince William Sound. Sea floor scarp heights range from 57 to 148 m on our crossing seismic profiles. As outlined in Liberty et al. (2013), the scarp lies at the margin of a large glacial channel, and we infer its height was enhanced by glacial erosion. Given its proximity to the thrust faults on Montague Island, we expected it to be a thrust fault. Instead, the seismic and bathymetric evidence, discussed below, indicate that it is a normal fault. Moreover, an M_w 4.8 normal fault earthquake at a depth of 11 km occurred nearly on the fault trace, on 9 August 2012 (AEIC event id: ak10531690), and it was followed by a M2.8 aftershock at a depth of 4 km (event id: ak10531730) (see Fig. 2). Earthquake hypocenter errors in this area are several kilometers (N. Ruppert, personal comm., 2012), and if this earthquake did not occur on the Montague Strait Fault, then it likely occurred on one of the similar, but smaller, faults nearby.

The Montague Strait Fault is one of a number of high-angle active faults between Knight and Montague Islands (Figs. 2 and 5). Some faults are sea-bottom lineations and we interpret other faults to lie where acoustic basement is adjacent to Holocene sediments. The overall structural style is of horsts and grabens (Fig. 5A). We infer the faults are likely normal faults based on back-tilting of strata in the footwall, and tilting of strata toward structural lows. The biggest problem for assessing the presence of faults and their sense of slip, is that the faults are most often at the margins, and not within, the Quaternary and Holocene sections. One particularly clear example is where the bathymetry shows a small (1.2 km) left stepping relay ramp along the Montague Strait Fault (Figs. 4 and 5). Seismic profiles demonstrate normal faulting along both strands and along subsidiary faults, but the relay ramp may be best explained by some component of strike-slip. The combination of the bathymetric expression of the Montague Strait Fault, the high-resolution seismic reflection data, and the 9 August 2012 earthquakes, lead us to conclude that there is a region of late Pleistocene–Holocene extension between Montague and Knight Islands. We collected high-resolution seismic data throughout Prince William Sound and normal faulting is limited to this region that extends eastward to Orca Bay near Cordova (Fig. 2; Finn, 2012). Lastly, the character of faulting, and possibly the Montague Strait

Fault, appears to change along strike to the southwest. A high-resolution seismic profile 25 km southwest of Prince William Sound, shows no evidence of normal faulting, and a fault in the along-strike location of the Montague Strait Fault is clearly a late-Quaternary, pre-Holocene, thrust fault (Liberty et al., 2013). The region of extension is limited to within Prince William Sound.

3. Patterns of long-term strain accumulation in Prince William Sound from thermochronology

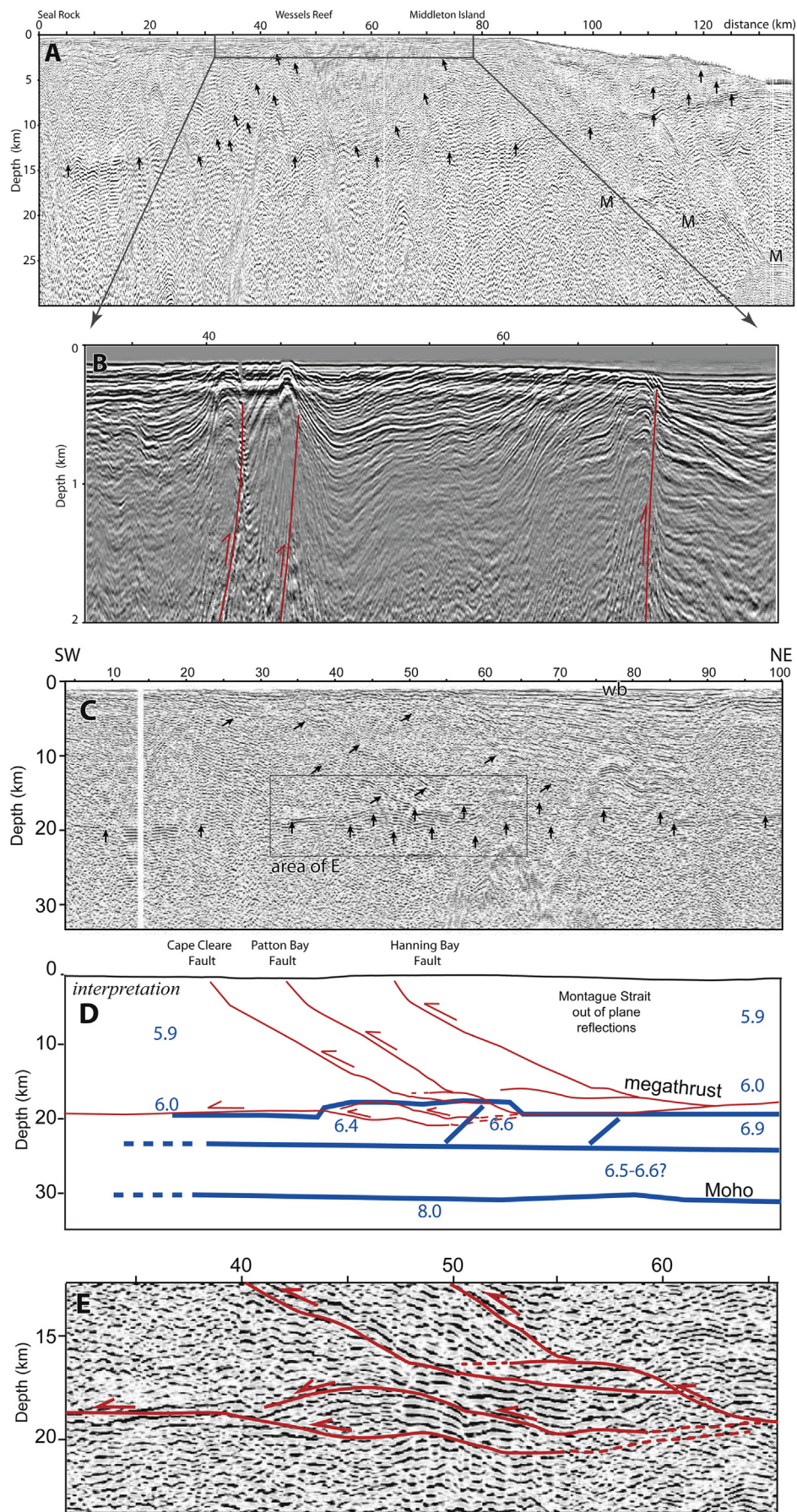
We use thermochronology data to assess long-term ($\geq 10^6$ years) rock uplift and exhumation as an indication of strain accumulation in the accretionary prism in Prince William Sound. The low-temperature thermochronology data shown in Fig. 6 are from Kveton (1989) and Buscher et al. (2009), but the majority of the ages ($n = 74$) are new data from Arkle et al. (2013) and Ferguson (2013), Ferguson et al. (2015); Table 1 that were collected to specifically address rock uplift and exhumation patterns in Prince William Sound and their relationships to subduction-related deformation. These publications discuss the details of sample analysis, methods, and interpretations. Most of the apatite fission-track (AFT) and/or apatite (U–Th)/He (AHe) sample locations in Fig. 6 form a broad swath across central and northern Prince William Sound (Arkle et al., 2013) and the region south of the Montague Strait Fault, principally on Montague and Hinchinbrook Islands (Ferguson, 2013; Ferguson et al., 2015). For this paper, it is useful to consider AFT ages as reflecting closure temperatures of approximately 110 °C and AHe ages reflecting cooling below modeled closure temperatures of approximately 65 °C.

Both the AFT and AHe datasets reveal similar patterns (Fig. 6). There are relatively older ages from central Prince William Sound (~10–20 Ma for AHe and ~20–40 Ma for AFT), with young ages surrounding northern Prince William Sound (~3–10 Ma for AHe and 10–16 Ma for AFT – see Arkle et al. (2013) for details). South of the Montague Strait Fault, nearly all the AHe ages are less than 5 Ma, with the youngest ages in all of Prince William Sound from Montague Island. On the southwestern part of the island there are four AHe ages less than 2 Ma and one that is 1.1 Ma. On the northeastern part of Montague Island and on Hinchinbrook Island, the ages are generally between 4 and 6 Ma (Fig. 6). These data demonstrate that the Montague Strait Fault has been an important structural boundary for exhumation for the last ~5 Ma. Lastly, we note that the oldest AFT age south of the Montague Strait Fault is 18.7 Ma from the east side of southern Montague Island. This sample is likely in the footwall of the Cape Cleare Fault. Although an AHe age of 5.8 Ma indicates these rocks experienced post-5-Ma exhumation, the older 18.7 Ma AFT age indicates the footwall of the Cape Cleare Fault experienced a smaller magnitude of post-5 Ma exhumation than the adjacent areas. This relationship underscores that the hanging wall of the Patton Bay megathrust splay system has been the locus of exhumation within the last 5 Ma.

The large-scale pattern in the thermochronology ages demonstrates rapid exhumation along the Patton Bay megathrust splay system and relatively slow exhumation (older AHe and AFT ages) in central Prince William Sound. This pattern of young exhumation ages is remarkably similar to the pattern of uplift in the 1964 earthquake (compare Fig. 6A and B to 6C), indicating uplift along megathrust splay faults in the 1964 earthquake reflects the long term pattern of rock uplift. The result also indicates little permanent rock uplift (<2.5 km) in the central part of the Prince William Sound for possibly 20,000 megathrust earthquake cycles.³ In contrast, there is focused rapid

² A Montague Strait Fault had previously been inferred by Nelson et al. (1985) east of Knight Island, and no specific structure was identified. S. Nelson (personal comm. 2013) stated that the angular discordance between bathymetric features on either side of Montague Strait motivated his inference of the fault. This insight is well founded, particularly given the newer bathymetry, which shows this discordance with much greater clarity and provides further justification for the fault. As the new multibeam data clearly define a particular structure, we assert that this scarp should be considered the Montague Strait Fault.

³ Assuming 600 years as the average recurrence interval of megathrust earthquakes (Carver and Plafker, 2008), and 10 Ma since the rocks passed through the AHe closure temperature, implies ~17,000 earthquakes. We round to 20,000 for simplicity.



exhumation underneath the high peaks of northern Prince William Sound, which is interpreted as related to underplating above the megathrust (Armstrong et al., 2011; Arkle et al., 2013), although that is not the focus of this paper.

A comparison of exhumation rates derived from the AFT and AHe methods indicates the rate of exhumation increased in the last 3 Ma (Ferguson, 2013; Ferguson et al., 2015). All but one of the 31 samples south of the Montague Strait Fault show a higher cooling rate from AHe closure to the surface than for cooling between AFT and AHe closure temperatures (Ferguson, 2013; Ferguson et al., 2015). Herman et al. (2013) recently summarized thermochronology data from around the world, and find that erosion rates have increases in the last 6 Ma, but particularly rapidly in the last 2 Ma. This increase in erosion rates was most pronounced in glaciated regions. Moreover, the beginning of the Pleistocene at ~2.6 Ma is marked by enhanced northern hemisphere glaciations (Lisiecki and Raymo, 2005; Clark et al., 2006; McClymont et al., 2013). Thus it seems likely that glaciation during this globally cool period enhanced tectonically driven rock uplift south of the Montague Strait Fault in the last 3 Ma.

A calculation of exhumation rate depends on geothermal gradient, which we can estimate for the Prince William Sound region based on heat flow measurements. Assuming a thermal conductivity of 2.5 W/mK for mixed sandstone and shale (Pollack et al., 2004) of Orca Group, a surface heat flow of 44 mW/m² (Blackwell and Richards, 2004) yields a background geothermal gradient of 18 °C/km. This estimate is very similar to the geotherm of 18.8 °C/km for the upper 3 km reported by Turner (1987) for the KSSD1 well located to the southwest off of Kodiak Island. This value is slightly lower than the present-day geothermal gradient of 22 °C/km for the Cook Inlet reported by Magoo (1986) and is in the range of gradients for “cold subduction zones” (Cloos, 1993). However, it is well known that the exhumation of rocks toward the surface causes geothermal gradients to increase (e.g., Kappelmeyer and Haenel, 1974; Powell et al., 1988; Ehlers, 2005). To correct for this advection effect, we apply a simple correction to the background geothermal gradient by assuming erosion durations consistent with sample ages and typical exhumation rates. Typical advection corrections result in about a 50% increase in geothermal gradient (Ehlers, 2005), resulting in a mean geothermal gradient of 24 °C/km – see Ferguson et al. (2015) for details. Using this advection corrected geotherm, an average calculated closure temperature of 66 °C (Ferguson, 2013; Ferguson et al., 2015), and a surface temperature of 0 °C (Péwé, 1975), we calculate exhumation rates as high as 2.8 mm/yr. As most samples were collected at or near sea level, the rock uplift, or erosion, rate is the same as exhumation. For the samples from northeastern Montague and Hinchinbrook Island the rate is about 0.7 mm/yr (Ferguson et al., 2015). These rates are in dramatic contrast to those north of the Montague Strait Fault, in central Prince William Sound, which average 0.2 mm/yr (Arkle et al., 2013). Thus, the most rapid exhumation in all of the Prince William Sound region is on

southwestern Montague Island. The topography of this island is not remarkable for Prince William Sound with peak elevations along its length of about 700 m, which is about the same height as the mountains on nearby Knight Island. In addition, although there is a gradient in exhumation ages along the length of Montague Island (Fig. 6), the consistent peak elevations indicate erosion is keeping pace with the variable exhumation rates (see Ferguson et al., 2015, for further discussion).

4. Structural context of rapid exhumation in southern Prince William Sound

Why is exhumation focused south of the Montague Strait fault? All the rocks in this region are mapped as the Paleocene-Eocene Orca Group of Grant and Higgins (1910; age modified by Plafker et al., 1985). These rocks experienced regional metamorphism up to lower-greenschist facies during accretionary processes (Nelson et al., 1985). The rocks were then intruded by anatetic granites around ~54 Ma and experienced additional regional metamorphism due to subduction of a spreading center beneath the continental margin (e.g. Bradley et al., 2003). This period was followed by intrusion of more granites of uncertain tectonic origin at ~38 Ma (Nelson et al., 1985), which likely included regional low-grade metamorphic effects.

Recent studies shed considerable light on the depositional age and thermal history of rocks in the area. Detrital zircon U/Pb studies on these Orca Group rocks have identified three belts of ages (Garver and Davidson, 2012; Hilbert-Wolf, 2012). To the northwest are rocks with maximum depositional zircon ages of 55–65 Ma (labeled ‘Orca Group’ on Fig. 6), in the middle is a narrow belt of rocks with maximum depositional ages of 37–45 Ma (labeled ‘Latouche belt’ on Fig. 6), and on Montague Island are rocks with maximum depositional ages of ~35 Ma (labeled ‘Montague belt’ on Fig. 6). Zircon fission track data (Kveton, 1989; Carlson, 2012) and paleomagnetic data (Bol, 1993) indicate that all the rocks northwest of the Montague Strait Fault experienced either, or both, of the ~54 and ~38 Ma thermal events, in contrast to the rocks on Montague Island that were deposited and accreted subsequent to these thermal episodes (Carlson, 2012; Garver and Davidson, 2012). Thus, the Montague Strait Fault divides these two rheologically distinct packages, which would be expected to deform rather differently. On Montague Island, zircon fission-track ages are unreset indicating these rocks could not have been heated to more than about 200 °C (Carlson, 2012). Thus the maximum amount of exhumation along the megathrust splay faults on Montague Island is about 8 km (Ferguson et al., 2015), which is about half the thickness of the accretionary prism above the subduction décollement. Moore and Meneghini (2007) described some of the rheological changes that occur in accretionary prisms. They noted that the development of upper plate rigidity is particularly important for seismogenesis. A prism thickness of greater than 3–5 km and particularly a high geothermal gradient, “accelerate metamorphism, cementation, and rigidification of the upper plate” (Moore and Meneghini, 2007, p. 308). The metamorphic and exhumational differences of the rocks

Fig. 3. Depth-migrated TACT deep seismic reflection profiles. Locations shown on Fig. 2. (A) TACT profile B showing the overall structure from the near the trench to the Hinchinbrook Entrance region. Arrows show locations of the décollement and the megathrust splay faults. Note that the megathrust splay faults have steeper dips upward. M indicates water bottom multiple. (B) Close up of the Wessels Reef and Middleton Island megathrust splay faults from the same TACT B profile, showing the near surface deformation and deflection of the sea floor. (C) TACT profile PWS. This line is about 20° from parallel to the strike of the faults and bedding in this area. Thus most of the reflections are related to out-of-plane reflections. Nonetheless, the line is important, because it images the Cape Cleare, Patton Bay, and Hanning Bay faults and indicates all intersect the megathrust separately. Fault plane reflections indicated by black arrows. (D) Interpretation of PWS line showing faults in red. The velocity structure of this line, from Brocher et al. (1994), is shown in blue. Velocities are listed in km/second. Note the reflector at ~20 km depth matches the change in refraction velocity from 6.0 to 6.9 km/s. Vertical exaggeration is ~1.5:1. (E) Blow up of interpreted duplex structure from area indicated in part (C). Red lines are faults, dashed where inferred. (For interpretation of the references to color in this figure legend, the reader is referred to the web version of this article.)

on either side of the Montague Straight fault are consistent with there being significant rheological differences between these two rock packages, which could be expected to localize deformation and faulting.

We constructed a northwest-trending schematic cross section across the Patton Bay megathrust splay fault system (Fig. 7). Constructing most of the profile is straightforward and well constrained. The TACT B and PWS seismic reflection profiles were used to guide interpretation of deep structure and the high-resolution seismic profiles to guide interpretation of shallower structures. We infer the Patton Bay thrust, the Hanning Bay thrust, and the Cape Cleare thrust faults are subparallel through most of the crust as indicated by the TACT PWS profile. We infer all three faults are more horizontal near the décollement and steeper near the surface, as indicated by the splays imaged on the TACT B profile (Fig. 3; Liberty et al., 2013). Any bulk horizontal shortening of the accretionary prism will result in additional material being thrust beneath the lowest part of the faults, which will result in rock uplift above the lowest part of the splay. Moreover, the TACT PWS profile shows underplating and transfer of material to the hanging wall in the region where the thrusts sole into the megathrust. The details of this region are not imaged well, so there is some latitude in interpretation.

The biggest uncertainty in constructing a cross section is the geometry of the Montague Strait fault at depth. We infer the Montague Strait normal fault has a dip of 61° to the SE, as indicated by the SE-dipping nodal plane of the 9 August 2012 earthquake. Given this, the Montague Strait Fault would intersect the Hanning Bay Fault at a depth between 10 and 15 km, but the specific structural configuration is underconstrained.

There are an abundance of observations of extension in accretionary prisms and contractional orogens that can shed some light as to the role and significance of the Montague Strait Fault. Some models for extension in contractional orogens relate to late stage extension, often related to gravitational collapse of high topography during orogeny (e.g. England, 1983; Malavieille et al., 1990). Other large normal faults in contractional orogens have been linked to late stage extension caused by duplexing at depth, such as the Brevard Zone in the Appalachians (Boyer and Elliott, 1982). However, other workers have documented normal faulting during contractional orogenesis (Platt, 1986; Carmignani and Kligfield, 1990; Wallis et al., 1993). Platt (1986) also argued in a more general sense that underplating of an accretionary wedge will cause the wedge to become oversteepened, resulting in extension of the wedge and exhumation of high-P and low-T metamorphic rocks. In the Apennines, both Carmignani and Kligfield (1990) and Wallis et al. (1993) provided evidence for upper crustal extension coeval with lower crustal duplexing, which is remarkably similar to the Alaskan story we present. However, these workers also found evidence for mid-crustal ductile extension in the Apennines, which has not been exposed or discovered or is absent in Alaska. Lastly, Wallis et al. (1993) also outlined general evidence for shortening during extension in accretionary wedges, with specific examples from the Calabrian arc of southern Italy and in the eastern Alps.

Theoretical, analog, and numerical models also predict extension in accretionary wedges. Dahlen (1984) showed that an oversteepened critically tapered coulomb wedge will undergo extension, but not how that would be structurally manifested. Wang and Hu (2006) considered the case of the critically tapered coulomb wedge thru the megathrust earthquake cycle, and they demonstrated that different parts of the wedge can change from compressional to extensional thru the earthquake cycle, and that both compressional and extensional stable

wedges can form the backstop to the deforming toe of the prism. An excellent example of what Wang and Hu (2006) predicted is the significant extension in the Kumano forearc basin landward of the megasplay fault in the Tonankai rupture area of the Nankai margin (Gulick et al., 2010). In this region, there are hundreds of normal faults related to extension above the megasplay. Thus, normal faults are found in the backstop –like the Montague Strait Fault.

Most analogue models of wedges require at least a small viscous horizon to produce extensional faulting during contraction (Buck and Sokoutis, 1994; Bonini et al., 2000; Haq and Davis, 2008; Gravelleau et al., 2012). Moreover, a numerical model by Willett (1999) requires at least a small shallow viscous layer to induce extension in the wedge, which seems consistent with the observations of Carmignani and Kligfield (1990) and Wallis et al. (1993) listed above. For Alaska, given the low geotherm and historical faulting in the 1964 earthquake, it seems unlikely that there is a viscous horizon, but it can not be ruled out. Conin et al. (2012) assessed the activity on subduction zone splay faults based on force-balance calculations. They "... suggest thrusting along the splay fault is generally conditioned by the growth of the accretionary wedge, or by the erosion of the hanging wall," which are both conditions that might fit southern Alaska. Their model also predicts extension in the hanging wall of a megathrust splay fault if there is moderate friction on both the splay and on the décollement. This model seems to fit our observations well, in that relatively low horizontal displacement of Middleton Island from the 1964 earthquake indicates low slip on the megathrust beneath, which indicates most horizontal slip, and presumably higher friction, was north of Middleton Island.

To summarize, although we still do not understand the specific structural linkage between the Montague Strait Fault and the Patton Bay splay fault system, there are a number of examples where extension has been documented in accretionary prisms or during contractional orogenesis, and both analog and theoretical models find circumstances where there is extension during contraction. Our study adds another example of extension in a contractional accretionary wedge.

What is driving the rock uplift and exhumation in the Montague Island region? Montague Island is approximately 160 km from the trench, along a part of the subduction décollement that is very shallowly dipping, and along which there is no large-scale change in dip. The subducting slab beneath Prince William Sound is composed of 15–30-km-thick oceanic plateau-like rocks of the Yakutat terrane, in contrast to 5–8-km-thick oceanic crust that is subducting to the southwest of Prince William Sound (Brocher et al., 1994; Eberhart-Phillips et al., 2006; Christeson et al., 2010; Fig. 1). The correlation between the location of the Yakutat flat slab and the region of rapid exhumation on Montague and Hinchinbrook Islands suggests there is a causal relationship between these factors. However, the region is northwest of the Yakutat terrane collision zone (e.g. Chapman et al., 2008; Fig. 1). On a regional map of AHe bedrock ages that includes our new data as well as the Yakutat collision zone (Fig. 8; Berger et al., 2008; Berger and Spotila, 2008; Falkowski et al., 2014), there are numerous AHe ages less than 5 Ma associated with the thin-skinned fold and thrust belt in the collision zone (Fig. 8; Enkelmann et al., 2010). The Yakutat collision zone is contiguous with the Alaska–Aleutian trench, as the terrane is being brought into the subduction zone. The young exhumation ages on Montague and Hinchinbrook Islands are along strike from, and synchronous with, the region of fast exhumation of the Yakutat collision zone (Falkowski et al., 2014). Both of these regions of fast exhumation lie in front of an older,

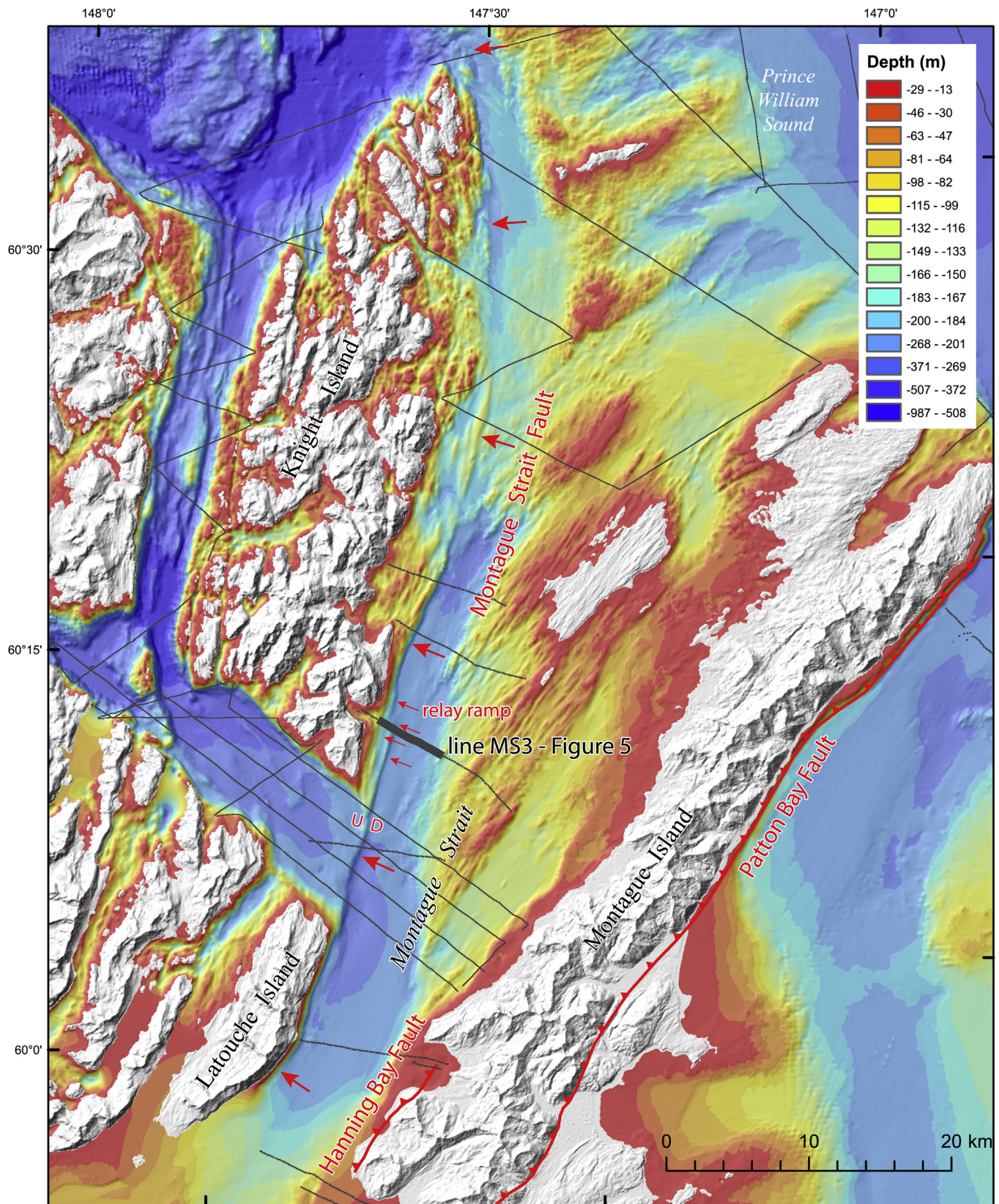


Fig. 4. Shaded topography and bathymetry map of region including Montague Strait fault and Patton Bay fault. The Montague Strait fault is southeast-side down and is delineated by red arrows to allow better viewing of scarp on bathymetry. The arrows at the north and south ends of the fault indicate the extent of the bathymetric expression of the fault. Sparker profiles we collected are shown with gray lines. Note the two parallel fault strands at the left stepping relay ramp, labeled and with small red arrows, in the trace of the fault crossed by line MS3, shown in Fig. 5. Multibeam bathymetry data from surveys collected by NOAA between 1998 and 2003. (For interpretation of the references to color in this figure legend, the reader is referred to the web version of this article.)

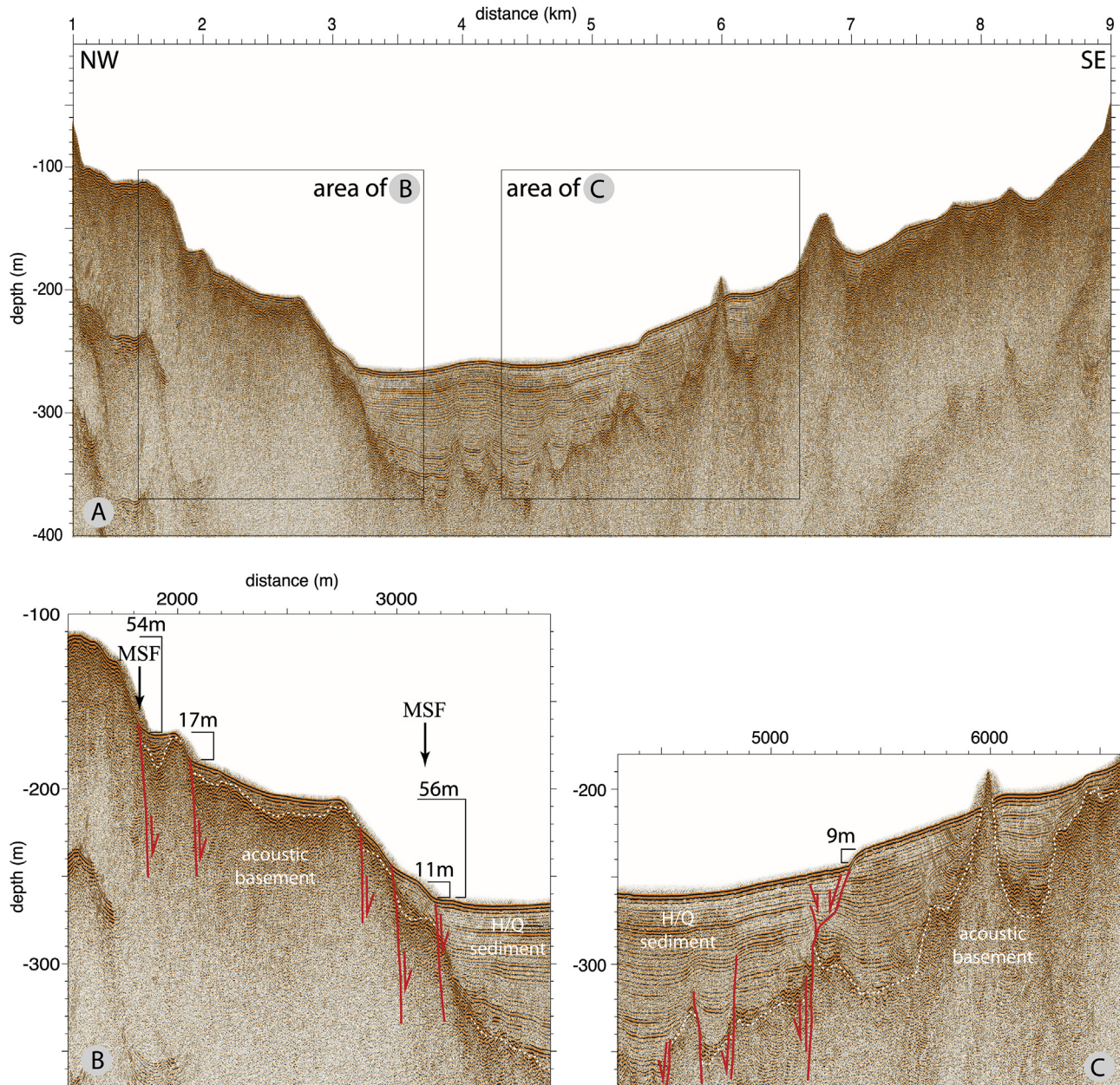


Fig. 5. Depth-converted sparker profile MS3, which crosses Montague Strait and the Montague Strait Fault. Position of line shown on Fig. 4. Velocity of sediments assumed to be 1600 m/s following Brocher et al. (1994). (A) Uninterpreted overview of central Montague Strait. (B) Southeast-dipping Montague Strait fault (denoted MSF) showing two strands of a relay ramp. The strands show normal faulting along the individual traces. Scarp heights, in meters, of individual scarps are shown with gray brackets, measured from bathymetry. Holocene and Quaternary sediment overlies acoustic basement. Imaging is degraded where there is a large velocity contrast, and thus offsets across faults between acoustic basement and the H/Q sediments should not be considered as precise. (C) Close up of normal faulting on the southeast side of Montague Strait. Multiple normal fault traces are seen at depth, but only one of these traces reaches the sea bottom.

more metamorphosed, and rigid crustal backstop, and thus the timing and style of exhumation in both places is similar. In summary, the Patton Bay megathrust splay fault system is characterized by rapid exhumation above a region of underplating and duplexing.

5. Variations in megathrust splay faults

The characteristics of the Patton Bay megathrust splay system are different than others, and we suggest there is significant intrinsic variability in subduction zone splay faults (Fig. 9). Other megathrust splay faults with historic rupture (Ecuador,

Tonankai, Maule, Sumatra) are not influenced by terrane (or other) collision,⁴ and these others are not topographically emergent. In fact, almost all others are below sea level. Most other megathrust splay faults, but not the Patton Bay, are located close to the updip limit of megathrust rupture (Park et al., 2002; Collot et al., 2008).

There are other significant differences between megathrust splay faults with historic rupture (Fig. 9). The Patton Bay

⁴ We do not consider progressive frontal accretion or subduction of an aseismic ridge as “collision.”

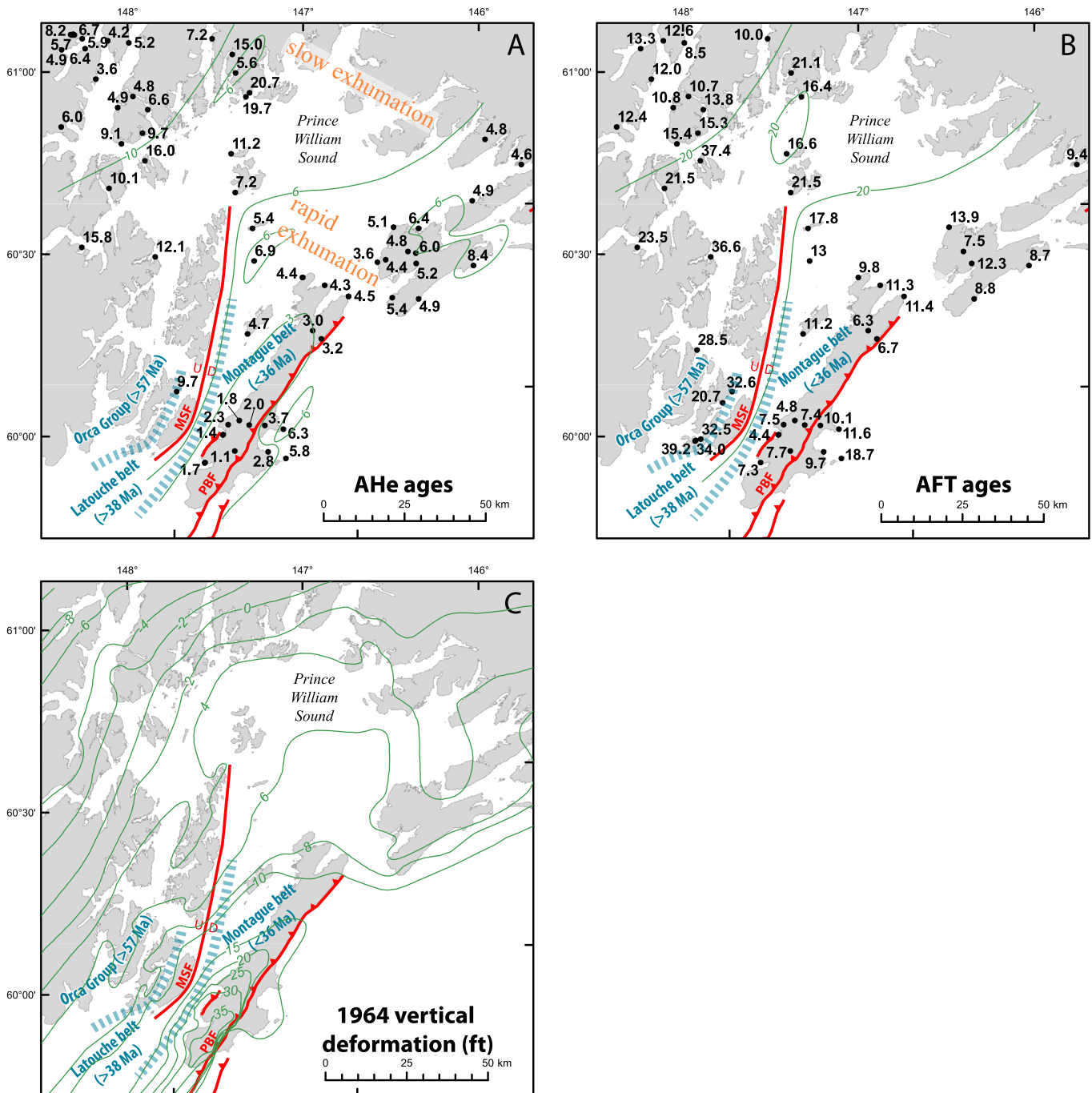


Fig. 6. Thermochronology, active faults, and 1964 deformation of the Prince William Sound region. Black dots show ages, in Ma, with contours of ages as thin black lines. Also shown are regions of rapid and slower exhumation, which are essentially the same with both AFT and AHe data. The northwestern region is discussed in Arkle et al. (2013). Active faults shown in red. Montague Strait fault, MSF; Patton Bay fault, PBF. In light blue are three belts of bedrock ages that have been defined in southwestern Prince William Sound based on the detrital zircon data of Carlson (2012). See text for additional discussion. The rocks north and west of the Montague Strait fault, with older exhumation ages, experienced both burial and contact metamorphism (Kveton, 1989; Hilbert-Wolf, 2012). This is in contrast to those rocks to the east and south, which are younger and are not metamorphosed. (Garver and Davidson, 2012; Hilbert-Wolf, 2012). A) Apatite (U–Th)/He (AHe) ages. B) Apatite fission track (AFT) ages. Age data from Buscher et al. (2008), Kveton (1989), Arkle et al. (2013) and Ferguson et al. (2015). C) Vertical deformation in the 1964 earthquake from Plafker (1969). Units are in feet as they were used in the original study. Positive values are uplift, negative values are subsidence. Note the remarkable correlation between the pattern of exhumation on the time span of millions of years, with the pattern coseismic deformation during the 1964 earthquake. (For interpretation of the references to color in this figure legend, the reader is referred to the web version of this article.)

Table 1

Summary of thermochronology data from Prince William Sound.

Sample	Latitude ^c	Longitude ^c	Elev. (m)	AHe (Ma) ^d	AFT (Ma) ^d	Rock type ^a	Reference ^b
PWS08-2	60.8465	-148.4285	500	6.0 ± 0.5	12.4 ± 1.5	Tg	A
PWS08-3	60.7864	-148.0963	0	9.1 ± 0.4	15.4 ± 1.6	Tg	A
PWS08-4	60.8925	-147.3416	0	20.7 ± 2.7		Tgg	A
PWS08-5	60.8830	-147.3648	0	19.7 ± 0.3	16.4 ± 3.0	Tgg	A
PWS08-6	60.9511	-147.4103	0	5.6 ± 0.6	21.1 ± 1.4	Tgg	A
PWS08-7	61.0029	-147.4182	0	15.0 ± 3.8		Tgg	A
PWS08-12	61.0510	-147.5250	0	7.2 ± 0.3	10.0 ± 1.0	Toc	A
PWS08-13	60.9136	-148.0062	0	4.8 ± 0.2	10.7 ± 1.0	Tg	A
PWS08-16	61.1428	-147.8330	0	4.0 ± 0.6	6.5 ± 0.8	Kvs	A
PWS08-21	61.1955	-147.7114	0	3.8 ± 0.7	6.5 ± 1.1	Kvs	A
PWS08-24	61.0716	-148.1214	0	4.2 ± 0.3	12.6 ± 1.8	Kvs	A
PWS08-31	60.9700	-148.2072	61	3.6 ± 0.6	12.0 ± 2.3	Tg	A
PWS08-32	60.5113	-148.3691	0	15.8 ± 0.4	23.5 ± 3.5	Tg	A
PWS06-1	60.6668	-148.1871	0	10.1 ± 1.2	21.5 ± 2.5	Tg	A
PWS06-2	60.4672	-147.9635	0	12.1 ± 2.3	36.6 ± 3.2	Tg	A
PWS06-3	59.9619	-147.6788	0	1.4 ± 0.1	4.4 ± 0.5	Tos	A
PWS06-5	60.0922	-147.9114	0	9.7 ± 0.9	32.6 ± 5.9	Toc	A
PWS06-9	60.7341	-147.9718	0	16.0 ± 5.0	37.4 ± 4.6	Tg	A
PWS06-10	60.8100	-147.9706	0	9.7 ± 1.4	15.3 ± 1.9	Tgg	A
PWS06-11	60.8734	-147.9294	0	6.6 ± 0.4	13.8 ± 1.6	Tgg	A
PWS06-12	60.8863	-148.0975	0	4.9 ± 0.1	10.8 ± 2.0	Tg	A
WH-PA06-1	60.7756	-148.7093	0	15.7 ± 1.7		Tfd	A
PWS09-6	61.2605	-147.6990	0	3.8 ± 0.5		Kvs	A
PWS09-7	61.1849	-147.8733	0	5.3 ± 0.5	8.4 ± 1.0	Kvs	A
PWS09-8	61.0617	-148.0014	0	5.2 ± 0.3	8.5 ± 1.3	Kvs	A
PWS08-12	61.0558	-148.2532	0	6.4 ± 0.04	13.3 ± 1.4	Kvs	A
PWS08-13	61.0586	-148.3879	0	4.9 ± 0.8		Kvs	A
PWS08-14	61.0977	-148.3292	1000	8.2 ± 0.8		Kvs	A
PWS08-15	61.0970	-148.3236	778	5.7 ± 1.5		Kvs	A
PWS08-16	61.0986	-148.3139	503	6.7 ± 0.2		Kvs	A
PWS08-17	61.0958	-148.3090	253	7.5 ± 0.7		Kvs	A
PWS08-18	61.0839	-148.2656	0	5.9 ± 0.1		Kvs	A
PWS10-1	61.3381	-147.5406	968	6.6 ± 0.8		Kvs	A
PWS10-3	61.4974	-147.8494	1752	7.6 ± 1.6		Kvs	A
PWS10-4	61.6675	-148.1294	1400	10.8 ± 1.3		Tfd	A
PWS10-5	61.6068	-148.1309	1374	8.4 ± 1.4		Kvs	A
PWS10-6	61.3893	-148.1269	1277	7.3 ± 1.0		Kvs	A
PWS10-7	61.2670	-148.5536	134	4.7 ± 0.9		Kvs	A
PWS10-8	60.7298	-147.4827	8	11.2 ± 1.9	16.6 ± 1.8	Tos	F
PWS10-9	60.6233	-147.4813	2	7.2 ± 1.4	21.5 ± 2.1	Tos	F
PWS10-10	60.5199	-147.4052	0	5.4 ± 1.1	17.8 ± 1.7	Tos	F
PWS10-11	60.4301	-147.4135	4	6.9 ± 1.4	13.0 ± 1.2	Tos	F
PWS10-12	60.2319	-147.4893	1	4.7 ± 0.5	11.2 ± 1.1	Tos	F
PWS08-6	59.9619	-147.6788	0	1.4 ± 0.2	4.4 ± 0.5	Tos	F
PWS10-13	59.8896	-147.7942	6	1.7 ± 0.6	7.3 ± 0.8	Tos	F
PWS10-14	60.3714	-147.1520	2	4.4 ± 0.2	9.8 ± 0.9	Tos	F
PWS10-15	60.3440	-147.0334	0	4.3 ± 0.1	11.3 ± 1.1	Tos	F
PWS10-16	60.3065	-146.9060	0	4.5 ± 0.9	11.4 ± 1.1	Tos	F
PWS11-1	59.8803	-147.3470	0	5.8 ± 0.9	18.7 ± 2.3	Tos	F
PWS11-2	59.9024	-147.4415	0	2.8 ± 0.1	9.7 ± 0.9	Tos	F
PWS11-3	59.9145	-147.6235	759	1.1 ± 0.4	7.7 ± 0.7	Tos	F
PWS11-4	59.9808	-147.5301	771	2.0 ± 0.6	4.8 ± 0.6	Tos	F
PWS11-5	59.9959	-147.5823	525	1.8 ± 0.6	7.4 ± 0.5	Tos	F
PWS11-6	59.9884	-147.6464	382	2.3 ± 0.2	7.5 ± 0.6	Tos	F
PWS11-7	59.9760	-147.4447	484	3.7 ± 0.2	10.1 ± 0.8	Tos	F
PWS11-8	59.9606	-147.3437	0	6.3 ± 1.0	11.6 ± 0.9	Tos	F
PWS11-9	60.1979	-147.0832	0	3.2 ± 0.8	6.7 ± 0.6	Tos	F
PWS11-10	60.2229	-147.1256	738	3.0 ± 0.7	6.3 ± 0.6	Tos	F
PWS10-17	60.2900	-146.6646	0	5.4 ± 0.8		Tos	F
PWS10-18	60.3907	-146.7257	0	3.6 ± 0.2	12.3 ± 1.1	Tos	F
PWS10-19	60.4817	-146.6135	13	5.1 ± 0.9	13.9 ± 1.0	Tos	F
PWS10-20	60.4717	-146.4744	0	6.4 ± 0.4		Tos	F
PWS11-11	60.4118	-146.5495	888	4.8 ± 0.7	7.5 ± 0.7	Tos	F
PWS11-12	60.3957	-146.6794	494	4.4 ± 0.6		Tos	F
PWS11-13	60.4044	-146.5061	443	6.0 ± 0.1		Tos	F
PWS11-14	60.3758	-146.5114	555	5.2 ± 0.6	12.3 ± 1.2	Tos	F
PWS11-15	60.2786	-146.5185	0	4.9 ± 1.3	8.8 ± 1.2	Tos	F
PWS11-16	60.3522	-146.1938	0	8.4 ± 1.8	8.7 ± 1.4	Tos	F
PWS10-21	60.5298	-146.1573	5	4.9 ± 0.2		Tos	F
PWS10-22	60.6124	-145.8570	0	4.6 ± 0.7	9.4 ± 0.9	Tos	F
PWS10-23	60.6034	-145.7414	5	4.1 ± 0.4	10.3 ± 1.1	Tos	F

^a Rock type abbreviations are: (Tg) Eocene–Oligocene intrusions; (Tgg) Sanak–Baranof intrusions; (Tfd) Tertiary felsic intrusions; (Toc & Tos) Paleocene–mid Eocene Orca Group conglomerate and sandstone; (Kvs) Cretaceous Valdez Group sandstone.

^b Source: A, [Arkle et al. \(2013\)](#); F, [Ferguson et al. \(2015\)](#).

^c Sample datums are reported in NAD 27.

^d Error for AFT and AHe ages are reported as 1σ and one standard error, respectively.

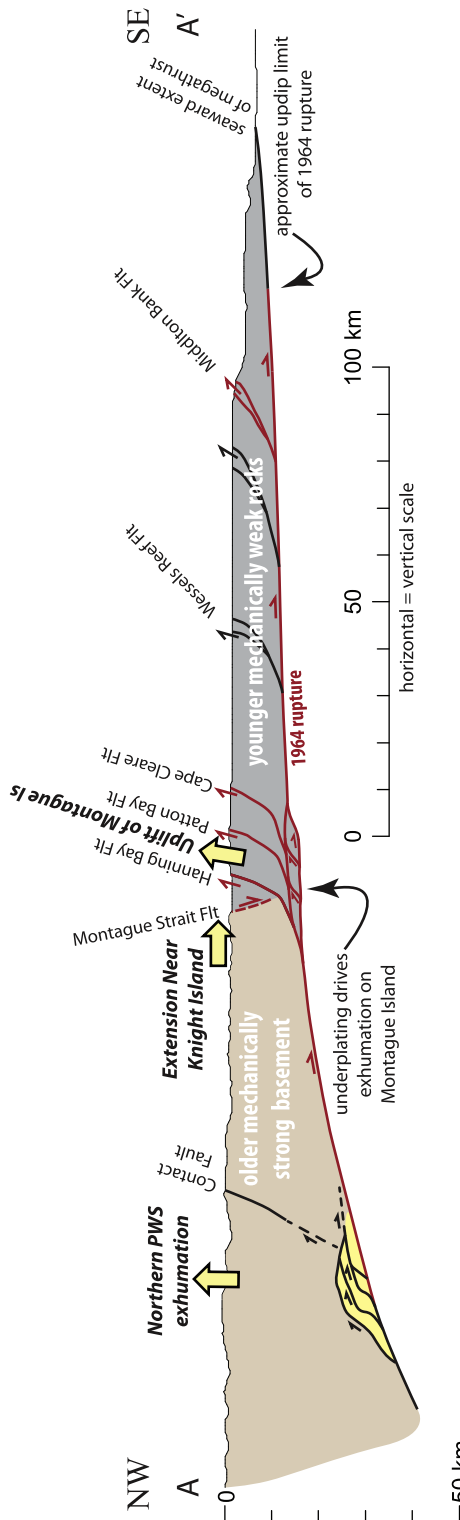


Fig. 7. Schematic cross section from the Alaska-Aleutian trench to the Kenai Peninsula highlighting structures that we infer result in exhumation. Cross section location shown on **Fig. 2**. Red lines show extent of rupture in the 1964 earthquake based on aftershocks, surface faulting, geodesy, Pfiffker's (1969) interpretation, and our interpretation of the structure. Underplated region beneath Montague Island is depicted as much thicker than it likely is for clarity. (For interpretation of the references to color in this figure legend, the reader is referred to the web version of this article.)

megathrust splay fault system is located about 160 km from the trench, where there is flat slab subduction at the edge of the Yakutat collision zone. Like the Patton Bay, a megathrust splay fault off of the Ecuador margin and another off the Tonankai part of the Nankai margin separates an older from a younger part of the accretionary complex (Park et al., 2002; Moore et al., 2007a,b; Collot et al., 2008). Like the Patton Bay, there is some normal faulting where the megathrust splay tip comes to the surface. However, unlike the more inland Patton Bay megathrust splay system, the Ecuador and Nankai megathrust splays are located near the top of the slope leading down to the trench. The most trenchward splay fault in Alaska near Middleton Island is in a similar structural position. The tip of the Nankai 'megasplay' is essentially becoming the primary décollement in the subduction zone and most slip occurs along this fault (Park et al., 2002; Moore et al., 2007a,b). Thus it is unlike the Alaska and Ecuador examples. A megathrust splay fault also ruptured in the 2010 M8.8 Maule earthquake in Chile (Melnick et al., 2012). This megathrust splay ruptured above a region of low coseismic slip as a large landward-vergent thrust, which is a growing anticline. At the surface, normal faulting was observed on the margins of the growing anticline. The variability in the characteristics among splay faults shown in **Fig. 9**, indicates that conditions for their formation are not particularly unique. We suggest these differences between the megathrust splay fault systems be noted, and more specifically, to use the pattern of long-term strain recorded by exhumation to illuminate the kinematics and duration of megathrust splay systems.

To summarize, in Alaska, we find evidence for focused exhumation along a megathrust splay fault system within the last 3 million years. Megathrust splay fault rupture in the 1964 earthquake was not a random event. Motion along this megathrust splay fault system appears to be driven by duplexing at the décollement. A comparison of megathrust splay fault systems around the world shows considerable variability in the tectonic setting and style of splay faulting, and at least some of these have a life span of several million years.

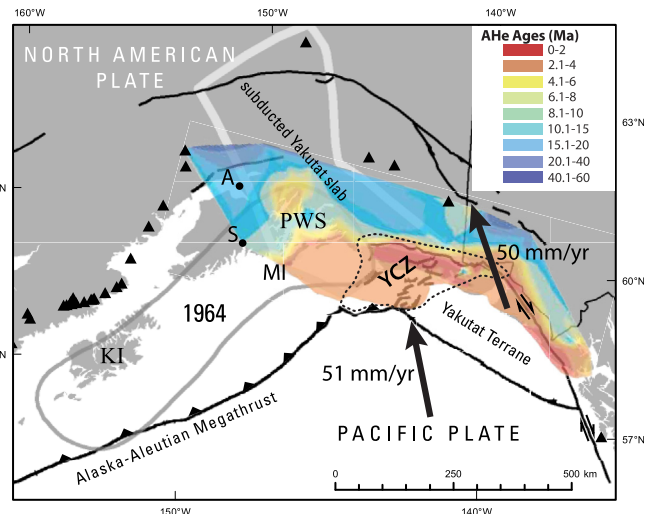


Fig. 8. Regional map of AHe exhumation ages from Ferguson (2013) superimposed on the regional tectonic setting shown in **Fig. 1**. Symbology is the same as **Fig. 1**. Thermochronology data are constrained to the land, although we infer the offshore region of the Yakutat terrane is also experiencing similarly young rapid exhumation, and it extends to Hinchinbrook and Montague Islands (MI) with exhumation focused along the megathrust splay faults. The Prince William Sound (PWS) region can thus be seen as an extension of the region of young exhumation in the Yakutat collision zone (YCZ).

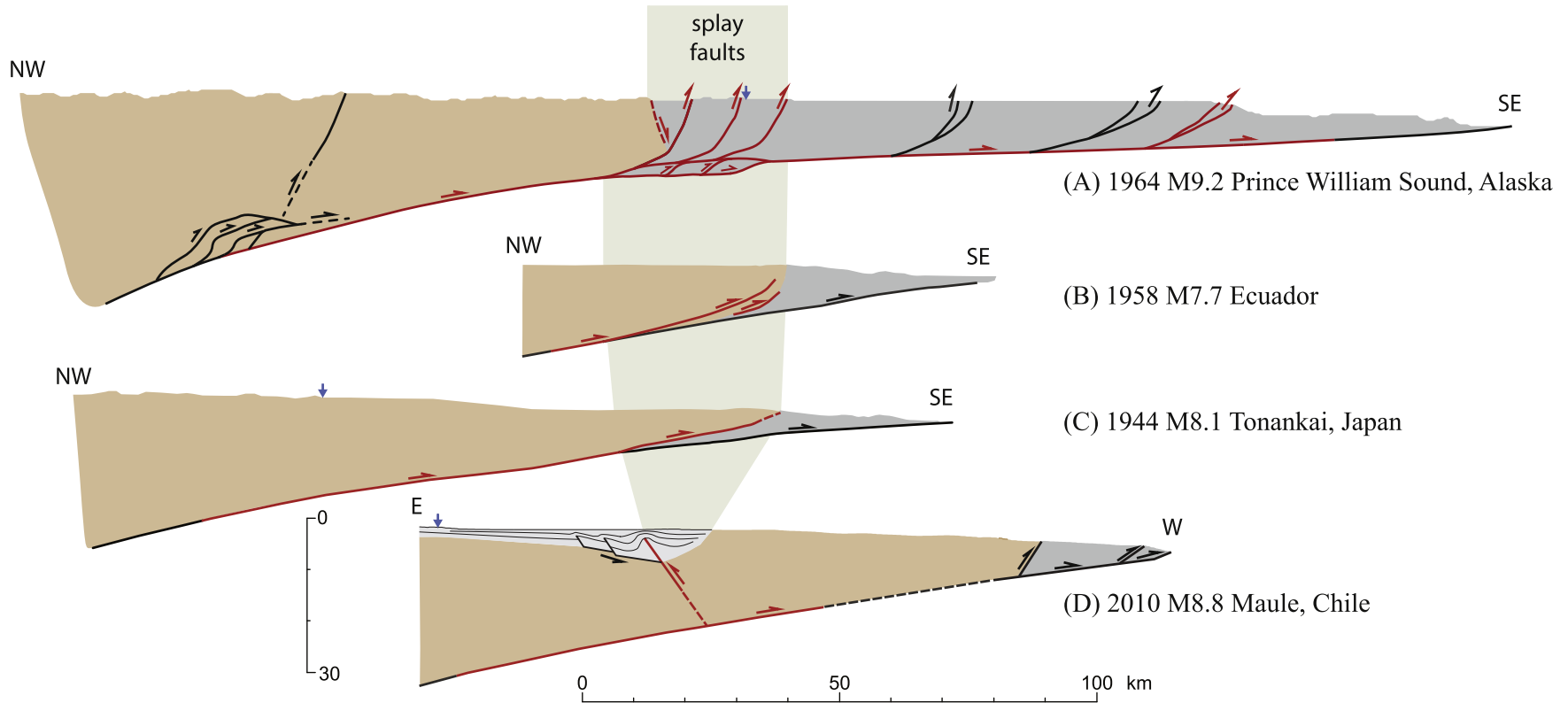


Fig. 9. Cross sections of historical megathrust splay fault ruptures. All cross sections shown at the same scale, with no vertical exaggeration, and all turned such that the trench is to the right. Black and red lines show active faults, with red lines showing faults inferred to have moved in the historic rupture. Down dip rupture extents from aftershocks. Tan regions show areas inferred to be mechanically stronger and gray regions show areas inferred to be mechanically weaker. Green polygon, behind cross sections, highlights the region of splay faults in each cross section. Blue arrows, where shown, give the location of the coastline. A) Prince William Sound, Alaska, region of the 1964 M9.2 rupture from Fig. 7 of this paper. B) Ecuador margin, from Collot et al. (2008). Red faults were identified by the limit of co-seismic slip in the 1958 M7.7 earthquake. Stronger and weaker regions were identified on the basis of seismic velocities derived from wide angle and pre-stack depth migration data. Profile is entirely offshore. C) Nankai, Japan, margin in the region of the 1944 Tonankai M8.1 earthquake. Structure from the trench to 70 km down dip from Park et al. (2002). Deeper structure from Kodaira et al. (2002). D) Splay fault geometry in central part of 2010 M8.8 rupture, from Melnick et al. (2012). (For interpretation of the references to color in this figure legend, the reader is referred to the web version of this article.)

Acknowledgments

Thanks to Captain Greg Snedgen of the USGS vessel *R/V Alaskan Gyre* for many long days of collecting seismic data. Thanks also to Keith Labay for help with drafting some figures. K. Farley and L. Hedges (Caltech) are thanked for (U–Th)/He analyses. Funding for Haeussler and Pratt from the USGS. Funding for Armstrong, Ferguson, and Arkle was provided by Donors of the Petroleum Research Fund administered by the American Chemical Society to Armstrong. Funding for Liberty and Finn came in part from U.S. Geological Survey National Earthquake Hazards Reduction Program award G11AP20143. A review of the manuscript by Richard Lease the three QSR reviewers, and Editor Ian Shennan greatly improved the clarity and focus.

References

- Arkle, J.C., Armstrong, P.A., Haeussler, P.J., Prior, M.G., Hartman, S., Sendziak, K.L., Brush, J.A., 2013. Focused exhumation in the syntaxis of the Chugach Mountains and Prince William Sound, Alaska. *Geol. Soc. Am. Bull.* 125 (5–6), 776–793. <http://dx.doi.org/10.1130/B30738.1>.
- Armstrong, P.A., Haeussler, P.J., Arkle, J.C., 2011. Styles and Causes of Deformation and Exhumation Related to Flat-slab Subduction of the Yakutat Microplate: a Low-temperature Thermochronometer Perspective. *Eos, Abs.* T33A-2385.
- Baba, T., Cummins, P.R., Hori, T., Kandeda, Y., 2006. High precision slip distribution of the 1944 Tonankai earthquake inferred from tsunami waveforms: possible slip on a splay fault. *Tectonophysics* 426, 119–134.
- Berger, A.L., Spotila, J.A., 2008. Denudation and deformation in a glaciated orogenic wedge: the St. Elias orogen, Alaska. *Geology* 36, 523–526. <http://dx.doi.org/10.1130/G24883A.1>.
- Blackwell, D.D., Richards, M., 2004. Geothermal Map of North America, American Association of Petroleum Geologists, Tulsa, 1 Sheet, Scale 1:6,500,000. Alaska portion at: <http://www.smu.edu/geothermal/2004NAMap/2004NAMap.htm> (last accessed 10.06.14).
- Boyer, S.E., Elliott, D., 1982. Thrust systems. *Am. Assoc. Pet. Geol. Bull.* 66, 1196–1230.
- Bradley, D., Kusky, T., Haeussler, P., Goldfarb, R., Miller, M., Dumoulin, J., Nelson, S.W., Karl, S., 2003. Geologic signature of early Tertiary ridge subduction in Alaska. In: Sisson, V.B., Roeske, S.M., Pavlis, T.L. (Eds.), *Geology of a Transpressional Orogen Developed During – Trench Interaction Along the North Pacific Margin*, pp. 19–49. *Geol. Soc. Am. Spec. Pap.* 371.
- Brocher, T.M., Fuis, G.S., Fisher, M.A., Plafker, G., Moses, M.J., Taber, J.J., Christensen, N.I., 1994. Mapping the megathrust beneath the northern Gulf of Alaska using wide-angle seismic data. *J. Geophys. Res.* 99 (B6), 11,663–11,685. <http://dx.doi.org/10.1029/94JB00111>.
- Berger, A.J., Spotila, J.A., Chapman, J., Pavlis, T.L., Enkelmann, E., Ruppert, N.A., Buscher, J.T., 2008. Architecture, kinematics, and exhumation of a convergent orogenic wedge: a thermochronological investigation of tectonic-climatic interactions within the central St. Elias Orogen, Alaska. *Earth Planet. Sci. Lett.* 270, 13–24. <http://dx.doi.org/10.1016/j.epsl.2008.02.034>.
- Bol, A.J., 1993. Overprint magnetizations in support of northward displacement of the Chugach–Prince William terrane, Alaska. *J. Geophys. Res.* 98 (B12), 22,389–22,400.
- Bonini, M., Sokoutis, D., Mulugeta, G., Katrivanos, E., 2000. Modelling hanging wall accommodation above rigid thrust ramps. *J. Struct. Geol.* 22 (8), 1165–1179.
- Buck, W.R., Sokoutis, D., 1994. Analogue model of gravitational collapse and surface extension during continental convergence. *Nature* 369 (6483), 737–740.
- Buscher, J.T., Berger, A.L., Spotila, J.A., 2008. Exhumation in the Chugach-Kenai mountain belt above the Aleutian subduction zone, southern Alaska. In: Freymueller, J.T., Haeussler, P.J., Wesson, R., Ekstrom, G. (Eds.), *Active Tectonics and Seismic Potential of Alaska*, Geophysical Monograph 179. American Geophysical Union, pp. 151–166. <http://dx.doi.org/10.1130/179GM08>.
- Carmignani, L., Kligfield, R., 1990. Crustal extension in the northern Apennines: the transition from compression to extension in the Alpi Apuane core complex. *Tectonics* 9, 1275–1303.
- Carlson, B.M., 2012. Cooling and provenance revealed through detrital zircon fission track dating of the Upper Cretaceous Valdez Group and Paleogene Orca Group in Western Prince William Sound, Alaska. In: *Proceedings from the 25th Keck Geology Consortium Undergraduate Research Symposium*, Amherst MA, pp. 8–16. ISSN# 1528-7491.
- Carver, G., Plafker, G., 2008. Paleoseismicity and neotectonics of the Aleutian subduction zone – an overview. In: Freymueller, J.T., Haeussler, P.J., Wesson, R.L., Ekström, G. (Eds.), *Active Tectonics and Seismic Potential of Alaska*, Geophysical Monograph 179. American Geophysical Union, pp. 43–63. ISBN 978-0-87590-444-3, AGU Code GM1794443.
- Chapman, J.B., Pavlis, T.L., Gulick, S., Berger, A., Lowe, L., Spotila, J., Bruhn, R., Vorkink, M., Koons, P., Barker, A., Picornell, C., Ridgway, K., Hallet, B., Jaeger, J., McCalpin, J., 2008. Neotectonics of the Yakutat collision: changes in deformation driving by mass redistribution. In: Freymueller, J.T., Haeussler, P.J., Wesson, R., Ekstrom, G. (Eds.), *Active Tectonics and Seismic Potential of Alaska*, Geophysical Monograph 179. American Geophysical Union, pp. 65–81. ISBN 978-0-87590-444-3, AGU Code GM1794443.
- Geophysical Monograph 179. American Geophysical Union, pp. 65–81. <http://dx.doi.org/10.1130/179GM04>.
- Christensen, D.H., Beck, S.L., 1994. The rupture process and tectonic implications of the Great 1964 Prince William Sound Earthquake. *Pure Appl. Geophys.* 142, 29–53.
- Christeson, G.L., Gulick, S.P.S., van Avendonk, H.J.A., Worthington, L.L., Reece, R.S., Pavlis, T.L., 2010. The Yakutat terrane: dramatic change in crustal thickness across the Transition fault, Alaska. *Geology* 38 (10), 895–898. <http://dx.doi.org/10.1130/G31170.1>.
- Clark, P.U., Archer, D., Pollard, D., Blum, J.D., Rial, J.A., Brovkin, V., Mix, A.C., Pisias, N.G., Roy, M., 2006. The middle Pleistocene transition: characteristics, mechanisms, and implications for long-term changes in atmospheric CO₂. *Quat. Sci. Rev.* 25, 3150–3184.
- Cloos, M., 1993. Lithospheric buoyancy and collisional orogenesis: subduction of oceanic plateaus, continental margins, island arcs, spreading ridges, and seamounts. *Geol. Soc. Am. Bull.* 105, 715–737.
- Collot, J.-Y., Agudelo, W., Ribodetti, A., Marcaillou, B., 2008. Origin of a crustal splay fault and its relation to the seismogenic zone and underplating at the erosional north Ecuador–south Colombia oceanic margin. *J. Geophys. Res.* 113, B12102. <http://dx.doi.org/10.1029/2008JB005691>.
- Conin, M., Henry, P., Godard, V., Bourlange, S., 2012. Splay fault slip in a subduction margin, a new model of evolution. *Earth Planet. Sci. Lett.* 341–344, 170–175.
- Dahlen, F.A., 1984. Noncohesive critical Coulomb wedges: an exact solution. *J. Geophys. Res.* 89, 10,125–10,133.
- Eberhart-Phillips, D., Christensen, D.H., Brocher, T.M., Hansen, R., Ruppert, N.A., Haeussler, P.J., Abers, G.A., 2006. Imaging the transition from Aleutian subduction to Yakutat collision in central Alaska, with local earthquakes and active source data. *J. Geophys. Res.* 111, B11303. <http://dx.doi.org/10.1029/2005JB004240>.
- Ehlers, T.A., 2005. Crustal thermal processes and the interpretation of thermochronometer data. *Rev. Min. Geochem.* 58, 315–350.
- Elliott, J.L., Larsen, C.F., Freymueller, J.T., Motyka, R.J., 2010. Tectonic block motion and glacial isostatic adjustment in southeast Alaska and adjacent Canada constrained by GPS measurements. *J. Geophys. Res.* 115, B09407. <http://dx.doi.org/10.1029/2009JB007139>.
- England, P.C., 1983. Some numerical investigations of large-scale continental deformation. In: Hsii, K.J. (Ed.), *Mountain Building Processes*. Academic Press, London, England, pp. 129–139.
- Enkelmann, E., Zeitler, P.K., Garver, J.I., Pavlis, T.L., Hooks, B.P., 2010. The thermochronological record of tectonic and surface process interaction at the Yakutat–North American collision zone in southeast Alaska. *Am. J. Sci.* 310, 231–260. <http://dx.doi.org/10.2475/04.2010.01>.
- Falkowski, S., Enkelmann, E., Ehlers, T.A., 2014. Constraining the area of rapid and deep-seated exhumation at the St. Elias syntaxis, Southeast Alaska, with detrital zircon fission-track analysis. *Tectonics* 33. <http://dx.doi.org/10.1002/2013TC003408>.
- Ferguson, K., 2013. *Rock Uplift Above the Subduction Megathrust at Montague and Hinchinbrook Islands, Prince William Sound, Alaska*. M.S. thesis, California State University Fullerton, 126 pp.
- Ferguson, K.M., Armstrong, P.A., Arkle, J.C., Haeussler, P.J., 2015. Focused rock uplift above the subduction décollement at Montague and Hinchinbrook Islands, Prince William Sound, Alaska. *Geosphere* 11. <http://dx.doi.org/10.1130/GES01036.1> (in press).
- Finn, S.P., 2012. *Megathrust Splay Fault Geometry in Prince William Sound, Alaska*. Boise State University, MS thesis, 148 pp.
- Garver, J.I., Davidson, C., 2012. Tectonic evolution of the Chugach–Prince William terrane, south-central Alaska. In: *Proceedings from the 25th Keck Geology Consortium Undergraduate Research Symposium*, Amherst MA, pp. 1–8. ISSN# 1528–7491.
- Grant, U.S., Higgins, D.F., 1910. Reconnaissance of the geology and mineral resources of Prince William Sound, Alaska. *U. S. Geol. Surv. Bull.* 443, 89 pp.
- Graveleau, F., Malavieille, J., Dominguez, S., 2012. Experimental modeling of orogenic wedges: a review. *Tectonophysics* 538–540, 1–66.
- Gulick, S.P.S., Bangs, N.L.B., Moore, G.F., Ashi, J., Martin, K.M., Sawyer, D.S., Tobin, H.J., Kuramoto, S., Taira, A., 2010. Rapid forearc basin uplift and megasplay fault development from 3D seismic images of Nankai Margin off Kii Peninsula, Japan. *Earth Planet. Sci. Lett.* <http://dx.doi.org/10.1016/j.epsl.2010.09.034>.
- Gutscher, M., Kukowski, N., Malavieille, J., Lallemand, S., 1998. Episodic imbricate thrusting and underplating: analog experiments and mechanical analysis applied to the Alaskan accretionary wedge. *J. Geophys. Res.* 103, 10,161–10,176.
- Haq, S.S.B., Davis, D.M., 2008. Extension during active collision in thin-skinned wedges: insights from laboratory experiments. *Geology* 36, 475–478.
- Heidarzadeh, M., Pirooz, M.D., Zaker, N.H., Yalciner, A.C., Mokhtari, M., Esmaeili, A., 2008. Historical tsunami in the Makran subduction zone off the southern coasts of Iran and Pakistan and results of numerical modeling. *Ocean Eng.* 35 (8&9), 774–786.
- Herman, F., Seward, D., Valla, P.G., Carter, A., Kohn, B., Willett, S.D., Ehlers, T.A., 2013. Worldwide acceleration of mountain erosion under a cooling climate. *Nature* 504, 423–428. <http://dx.doi.org/10.1038/nature12877>.
- Hilbert-Holter, H.L., 2012. A U/Pb detrital zircon provenance of the flysch of the Paleogene Orca Group, Chugach–Prince William terrane, Alaska. In: *Proceedings from the 25th Keck Geology Consortium Undergraduate Research Symposium*, Amherst MA, pp. 23–32. ISSN# 1528–7491.
- Holdahl, S.R., Sauber, J., 1994. Coseismic slip in the 1964 Prince William Sound earthquake: new geodetic inversion. *Pure Appl. Geophys.* 142, 55–82.

- Ichinose, G., Somerville, P., Thio, H.K., Graves, R., O'Connell, D., 2007. Rupture process of the 1964 Prince William sound, Alaska, earthquake from the combined inversion of seismic, tsunami, and geodetic data. *J. Geophys. Res.* 112, B07306. <http://dx.doi.org/10.1029/2006JB004728>.
- Johnson, J., Satake, K., Holdahl, S.R., Sauber, J., 1996. The 1964 Prince William Sound earthquake: joint inversion of tsunami and geodetic data. *J. Geophys. Res.* 101, 523–532.
- Kappelmeyer, G., Haenel, R., 1974. *Geothermics*. Gebruder Borntraege, Berlin.
- Kodaira, S., Kurashimo, E., Park, J.-O., Takahashi, N., Nakanishi, A., Miura, S., Iwasaki, T., Hirata, N., Ito, K., Kaneda, Y., 2002. Structural factors controlling the rupture process of a megathrust earthquake at the Nankai trough seismogenic zone. *Geophys. J. Int.* 149, 815–835.
- Kveton, K.J., 1989. *Structure, Thermochronology, Provenance and Tectonic History of the Orca Group in Southwestern Prince William Sound, Alaska*. Ph.D. dissertation, University of Washington, 173 pp.
- Liberty, L.M., Finn, S.P., Haeussler, P.J., Pratt, T.L., Peterson, A., 2013. Megathrust splay faults at the focus of the Prince William Sound asperity, Alaska. *J. Geophys. Res.* 118, 1–14. <http://dx.doi.org/10.1002/jgrb.50372>.
- Lisiecki, L.E., Raymo, M.E., 2005. A Pliocene–Pleistocene stack of 57 globally distributed benthic d18O records. *Paleoceanography* 20, PA1003. <http://dx.doi.org/10.1029/2004PA001071>.
- Malavieille, J., Guihot, P., Costa, S., Lardeaux, J.M., Gardien, V., 1990. Collapse of the thickened Variscan crust in the French Massif Central: Mont Pilat extensional shear zone and St. Etienne Late Carboniferous basin. *Tectonophysics* 177, 139–149.
- Magoon, L.B., 1986. Present-day geothermal gradient. In: Magoon, L.B. (Ed.), *Geologic Studies of the Lower Cook Inlet COST No. 1 Well, Alaska Outer Continental Shelf*. U.S. Geol. Surv. Bull. 1596, 41–46.
- McCliment, E.L., Sodian, S.M., Rosell-Melé, A., Rosenthal, Y., 2013. Pleistocene sea-surface temperature evolution: early cooling, delayed glacial intensification, and implications for the mid-Pleistocene climate transition. *Earth Sci. Rev.* 123, 173–193.
- Melnick, D., Moreno, M., Motagh, M., Cisternas, M., Wesson, R.L., 2012. Splay Fault Slip During the M_w8.8 2010 Maule Chile Earthquake, vol. 40, pp. 251–254. <http://dx.doi.org/10.1130/G32712.1>.
- Moore, J.C., Diebold, J., Fisher, M.A., Sample, J., Brocher, T., Talwani, M., Ewing, J., von Huene, R., Rowe, C., Stone, D., Stevens, C., Sawyer, D., 1991. EDGE deep seismic reflection transect of the eastern Aleutian arc-trench layered lower crust reveals underplating and continental growth. *Geology* 19, 420–424.
- Moore, G.F., Bangs, N.L., Taira, A., Kuramoto, S., Pangborn, E., Tobin, H.J., 2007a. Three-dimensional splay fault geometry and implications for tsunami generation. *Science* 318, 1128–1131.
- Moore, J.C., Rowe, C.D., Meneghini, F., 2007b. How can accretionary prisms elucidate seismogenesis in subduction zones? In: Dixon, T. (Ed.), *Proceedings from the Seismogenic Zone Theoretical Institute, Snowbird, Utah, March 2003*. Columbia University Press, pp. 288–315.
- Nelson, S.W., Dumoulin, J.A., Miller, M.L., 1985. *Geologic Map of the Chugach National Forest, Alaska*. U.S. Geol. Surv. Misc. Field Studies Map MF-1645B, scale 1: 250,000, 16 pp.
- Okal, E.A., Borrero, J.C., 2011. The ‘tsunami earthquake’ of 1932 June 22 in Manzanillo, Mexico: seismological study and tsunami simulations. *Geophys. J. Int.* 187, 1443–1459. <http://dx.doi.org/10.1111/j.1365-246X.2011.05199.x>.
- Park, J.-O., Tsuru, T., Kodaira, S., Nakanishi, A., Miura, S., Kaneda, Y., Kono, Y., 2000. Out-of-sequence thrust faults developed in the coseismic slip zone of the 1946 Nankai earthquake (Mw = 8.2) off Shikoku, southwest Japan. *Geophys. Res. Lett.* 27, 1033–1036. <http://dx.doi.org/10.1029/1999GL008443>.
- Park, J.-O., Tsuru, T., Kodaira, S., Cummins, P.R., Kaneda, Y., 2002. Splay fault branching along the Nankai subduction zone. *Science* 297, 1157–1160. <http://dx.doi.org/10.1126/science.1074111>.
- Pewé, T.L., 1975. *Quaternary Geology of Alaska*. U.S. Geol. Surv. Prof. Pap. 835, 145 pp.
- Plafker, G., 1967. Surface Faults on Montague Island Associated with the 1964 Alaska Earthquake. *U.S. Geol. Surv. Prof. Pap.* 543-G, 42 pp.
- Plafker, G., 1969. Tectonics of the March 27, 1964 Alaska Earthquake. *U.S. Geol. Surv. Prof. Pap.* 543-I, 74 pp.
- Plafker, G., Gilpin, L.M., Lahr, J.C., 1994. Neotectonic map of Alaska. In: Plafker, G., Berg, H.C. (Eds.), *The Geology of Alaska*. Geol. Soc. Am., the Geology of North America, G-1, pl. 12, Scale 1:2,500,000.
- Plafker, G., Keller, G., Nelson, S.W., Dumoulin, J.A., Miller, M.L., 1985. Summary of data on the age of the Orca Group, Alaska. In: Bartsch-Winkler, S. (Ed.), *The United States Geological Survey in Alaska: Accomplishments During 1984*. U.S. Geol. Surv. Circ. 967, 74–76.
- Platt, J.P., 1986. Dynamics of orogenic wedges and the uplift of high pressure metamorphic rocks. *Geol. Soc. Am. Bull.* 97, 1037–1053.
- Plattner, C., Malservisi, R., Dixon, T.H., Lafemina, P., Sella, G.F., Fletcher, J., Suarez-Vidal, F., 2007. New constraints on relative motion between the Pacific Plate and Baja California microplate (Mexico) from GPS measurements. *Geophys. J. Int.* 170, 1373–1380. <http://dx.doi.org/10.1111/j.1365-246X.2007.03494.x>.
- Powell, W.G., Chapman, D.S., Balling, N., Beck, A.E., 1988. Continental heat flow density. In: Haenel, R., Rybach, L., Stegenga, L. (Eds.), *Handbook of Terrestrial Heat-flow Density Determinations*, pp. 167–222.
- Suito, H., Freymueller, J., 2009. A viscoelastic and afterslip postseismic deformation model for the 1964 Alaska earthquake. *J. Geophys. Res.* 114, B11404. <http://dx.doi.org/10.1029/2008JB005954>.
- Suleiman, E., Nicolsky, D.J., Haeussler, P.J., Hansen, R., 2010. Combined effects of tectonic and landslide-generated tsunami runup at Sward, Alaska during the Mw9.2 1964 earthquake. *Pure Appl. Geophys.* <http://dx.doi.org/10.1007/s00024-010-0228-4>.
- Turner, R.F. (Ed.), 1987. *Geological and Operational Summary Kodiak Shelf Stratigraphic Test Wells, Western Gulf of Alaska*. U.S. Dept. of the Interior, Minerals Management Service, 341 pp.
- Wallis, S.R., Platt, J.P., Knott, S.D., 1993. Recognition of syn-convergence extension in accretionary wedges with examples from the Calabrian arc and the eastern Alps. *Am. J. Sci.* 293, 463–495.
- Wang, K., Hu, Y., 2006. Accretionary prisms in subduction earthquake cycles: the theory of dynamic Coulomb wedge. *J. Geophys. Res.* 111, B06410. <http://dx.doi.org/10.1029/2005JB004094>.
- Wendt, J., Oblesky, D.D., Geist, E.L., 2009. Tsunamis and splay fault dynamics. *Geophys. Res. Lett.* 36, L15303. <http://dx.doi.org/10.1029/2009GL038295>.
- Willett, S.D., 1999. Rheological dependence of extension in wedge models of convergent orogens. *Tectonophysics* 305, 419–435.
- Wilson, B.W., Tørum, A., 1972. Effects of the tsunamis: an engineering study. In: *The Great Alaska Earthquake of 1964. Oceanography and Coastal Engineering*, National Academy of Sciences, pp. 361–523.